

the corresponding surface element provides the predicted gamma-ray flux at any given altitude.

[55] PRF(d) exhibits the expected behavior, as it is maximum at the sub-nadir point and goes to zero at the limb, where $\cos(d/R_M) = 1/(1 + h/R_M)$. The integral of the PRF over the planet surface is proportional to the solid angle subtended by the planet at altitude h . A comparison of the results of the PRF so calculated to the experimentally determined PRF for the Lunar Prospector GRS at 30 km altitude [Lawrence *et al.*, 2003] and the simulated PRF for the Mars Odyssey GRS at 400 km [Boynton *et al.*, 2007] altitude shows agreements. The PRF also has the expected behavior at large altitudes ($h \gg R_M$), where the subtended solid angle is small and the detector-incident gamma rays are parallel. These tests provided the confidence necessary to utilize this PRF over the full range of altitudes in the low-altitude data set (200–2000 km).

Appendix B: Correlation Between Spacecraft Ephemeris and GRS Measurements

B1. GRS Measurement Geometry

[56] During MESSENGER's primary mission, the spacecraft orbited Mercury in a highly eccentric, near polar orbit with a period of 12 h (see Figure B1a). This orbit, in conjunction with the altitude dependence of the GRS signal (equation (1)), limited the spatial coverage of the GRS measurements to regions north of -20° latitude. This orbit also results in a double-valued correlation between the spacecraft altitude and the sub-nadir latitude (Figure B1b). As a result, the spatial resolution and statistical significance

of the measurements have a latitudinal dependence, with higher spatial resolution and sensitivity at northern latitudes. This effect necessitated the use of varying pixel sizes in the K abundance map (Figure 8) in order to maintain low statistical errors for each pixel.

[57] The thermal conditions at the surface, particularly the presence of hot poles at longitudes 0° and 180° , frequently necessitated the use of off-nadir pointing over these regions, which includes the Caloris basin. This off-nadir pointing can potentially impact the measured gamma-ray count rates, as measurements taken at large nadir angles have lower detection efficiencies (see Figures A4 and A5). Our map of K abundances, which has the highest values in the far north and low values over the hot poles, could possibly be attributed to the nature of the MESSENGER orbit and spacecraft attitude if the data were not properly corrected.

[58] Evidence that these observational biases have not influenced the results comes from two sources. The first is the 1779-keV Si and 6129-keV O gamma-ray count rate maps. These gamma rays, particularly the 1779-keV line, are subject to the same measurement correlations as the 1461-keV K gamma ray. The uniform count rate maps for the 1779-keV and 6129-keV gamma rays are taken as evidence that the corrections described here have fully removed the effects of the measurement correlations from this analysis, on the grounds that correlations would otherwise be observed between these gamma rays and spacecraft attitude for each pixel. The second piece of evidence comes from plotting the K abundance versus the measurement time, average nadir angle, and average altitude for each pixel. In all cases, no correlation was found between the derived K abundance and the measurement parameter.

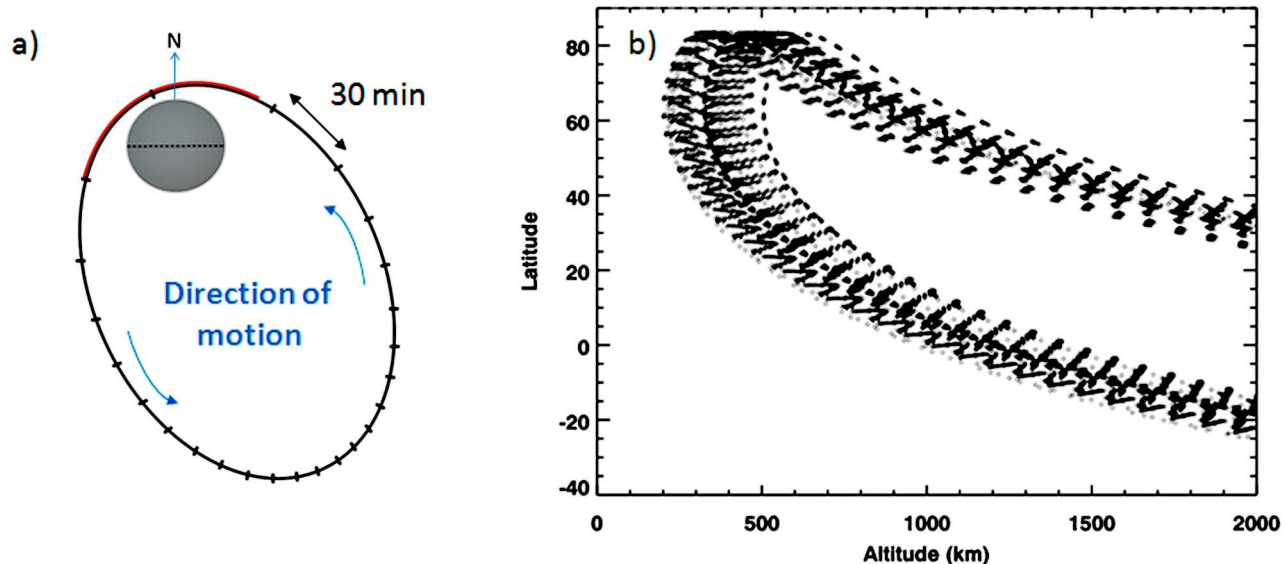


Figure B1. (a) The near-polar, highly eccentric orbit of the MESSENGER spacecraft during its primary mission, with tick marks at 30-min time intervals and blue arrows indicating the direction of spacecraft motion. The orbit ranges from a minimum periapsis altitude of 200 km to a maximum apoapsis altitude of 15,500 km. The red highlighted segment of the orbit illustrates the low-altitude (<2000 km) portion. (b) The latitude of the spacecraft as a function of altitude for all data acquired from 24 March to 28 September 2011. There are two branches in this representation of the orbit, which results in a latitude-dependent signal strength and spatial resolution.